Published in final edited form as:
Stem Cells. 2014 January ; 32(1): 70–84. doi:10.1002/stem.1520.

Molecular Diversity Subdivides the Adult Forebrain Neural Stem Cell Population

Claudio Giachino[a,b], **Onur Basak**[b], **Sebastian Lugert**[a,b], **Philip Knuckles**[b], **Kirsten Obernier**[c], **Roberto Fiorelli**[d], **Stephan Frank**[e], **Olivier Raineteau**[d], **Arturo Alvarez–Buylla**[c], and **Verdon Taylor**[a,b]

[a]Embryology and Stem Cell Biology, Department of Biomedicine, University of Basel, Basel, Switzerland [b]Department of Molecular Embryology, Max Planck Institute of Immunobiology, Freiburg, Germany [c]Department of Neurological Surgery, University of California San Francisco, San Francisco, California, USA [d]Institut fur Hirnforschung, Universitat Zurich, Zurich, Switzerland [e]Division of Neuropathology, Institute of Pathology, University of Basel, Basel, Switzerland

Abstract

Neural stem cells (NSCs) in the ventricular domain of the subventricular zone (V-SVZ) of rodents produce neurons throughout life while those in humans become largely inactive or may be lost during infancy. Most adult NSCs are quiescent, express glial markers, and depend on Notch signaling for their self-renewal and the generation of neurons. Using genetic markers and lineage tracing, we identified subpopulations of adult V-SVZ NSCs (type 1, 2, and 3) indicating a striking heterogeneity including activated, brain lipid binding protein (BLBP, FABP7) expressing stem cells. $BLBP^+$ NSCs are mitotically active components of pinwheel structures in the lateral ventricle walls and persistently generate neurons in adulthood. $BLBP^+$ NSCs express epidermal growth factor (EGF) receptor, proliferate in response to EGF, and are a major clonogenic population in the SVZ. We also find BLBP expressed by proliferative ventricular and sub-ventricular progenitors in the fetal and postnatal human brain. Loss of $BLBP^+$ stem/progenitor cells correlates with reduced neurogenesis in aging rodents and postnatal humans. These findings of molecular heterogeneity and proliferative differences subdivide the NSC population and have implications for neurogenesis in the forebrain of mammals during aging.

Correspondence: Verdon Taylor, Ph.D., Embryology and Stem Cell Biology, Department of Biomedicine, University of Basel, Mattenstrasse 28, CH-4058 Basel, Switzerland. Telephone: +41 616953091; Fax: +41 616953090; verdon.taylor@unibas.ch.

Disclosure of Potential Conflicts of Interest
The authors indicate no potential conflicts of interest.

Author Contributions
C.G. and O.B.: conception and design, collection and assembly of data, data analysis and interpretation, manuscript writing, and final approval of manuscript, S.L. and P.K.: collection and assembly of data and data analysis and interpretation; K.O., S.F. O.R., and A.A-B.: provision of study material and manuscript writing; R.F.: provision of study material; V.T.: conception and design, financial support, assembly of data, data analysis and interpretation, manuscript writing, and final approval of manuscript. C.G. and O.B. contributed equally to this article.

Keywords

Neurogenesis; Subventricular zone; Neural stem cells; Aging

Introduction

Somatic stem cells replace and replenish cells in many adult tissues [1, 2]. Adult neural stem cells (NSCs) (B1 cells) reside in the ventricular domain of the subventricular zone (V-SVZ) of the lateral ventricle wall in rodents and share ultrastructural and antigenic features with astrocytes [3, 4]. Some B1 cells in the adult V-SVZ are mitotically active and others may represent a quiescent reservoir for regenerating the neurogenic niche [3–7]. Activated B1 cells divide and likely undergo asymmetric cell divisions to self-renew and generate committed transient amplifying progenitors (TAPs—C cells). C cells are a transient, mitotically active population dividing frequently to generate neuroblasts (A cells) that migrate through the rostral migratory stream (RMS) to the olfactory bulb (OB) [8, 9]. The V-SVZ astrocytes constitute a heterogeneous cell population and only a subpopulation of these are bona fide NSCs, while others are niche cells [10–13]. Discrimination of NSCs from non-neurogenic astrocytes and quiescent NSCs from activated NSCs in the V-SVZ has proven difficult partially due to a lack of markers.

Notch signaling regulates cell fate throughout the animal kingdom [14, 15]. Notch signaling controls NSC differentiation and inhibits neurogenesis through activation of *Hes* genes [7, 16–23]. Here we addressed NSC heterogeneity within the Notch dependent V-SVZ stem cell pool. We identified adult NSC populations with distinctive antigenic and mitotic properties that are marked by the Notch target Hes5 and express glial fibrillary acidic protein (GFAP) or brain lipid binding protein (BLBP) and epidermal growth factor receptor (EGFR) or a combination of these. We characterize *Hes5*$^{+}$BLBP^{+}cells, a novel V-SVZ cell type, and show them to be colony forming in vitro and a resident long-term neurogenic population in vivo. These BLBP^{+} NSCs are S-phase label-retaining cells and can transit between mitotic activity and quiescence. However, they are more proliferative than anticipated consistent with being activated stem cells. *Hes5*$^{+}$BLBP^{+} cells are dramatically depleted during aging but express receptors for growth factors that stimulate NSC self-renewal. In humans, the presence of BLBP^{+} cells correlates with mitotic activity and neurogenesis, and BLBP^{+}cells are found within the astrocytic ribbon NSC niche of the postnatal human brain.

Materials and Methods

Animals, Generation of *Hes5::CreER*^{T2} and *Blbp::mCherry* Transgenic Mice

Hes5::GFP, *Hes5::CreER*^{T2}, *GFAP::CreER*^{T2}, *Rosa26::YFP*, and *Rosa-CAG::GFP* mice have been described elsewhere [16, 24–27]. *Blbp::mCherry* transgenic mice were generated by isolation of a 7.6 kb fragment of the mouse *Blbp* gene from a BAC including 4 kb of promoter region. An mCherry cDNA was inserted in-frame into a modified translation start site of the BLBP coding region which included a perfected Kozak translation initiation sequence (CCACCATG). The offsprings of 10 founder *Blbp::mCherry* mice were analyzed,

and three lines established on a C57/Bl6 genetic background, all showing comparable expression profiles.

5-Bromo-Deoxyuridine Administration and Tamoxifen Treatment

Adult mice 8–10 weeks of age were used in the experiments. *GFAP::CreER^{T2}* and *Hes5::CreER^{T2}* mice were injected daily intraperitoneal (i.p.) with 2 mg Tamoxifen (TAM) in corn oil (100 μL of 20 mg/mL) for five consecutive days and killed 1 or 10 days (*GFAP::CreER^{T2}*) or 1, 21 or 100 days (*Hes5::CreER^{T2}*) after the end of the treatment. 5-Bromo-deoxyuridine (BrdU) was administered to adult *Hes5::GFP* mice in the drinking water (0.8 mg/mL) for 15 consecutive days. The mice were killed either directly after the 15-day BrdU treatment or following a 30-day chase. Alternatively, *Hes5::GFP* mice received BrdU intraperitoneally (50 mg/kg b.wt.) and were killed 2 hours after injection. Mice were maintained on a 12-hour day/night cycle with food and water ad libitum under specified pathogen free conditions and according to Max Planck Institutional and German Federal regulations and under license numbers 35/9185.81/G-09/19 (Ethical Commission Freiburg, Germany).

Tissue Preparation for Immunochemical Staining

Animals were perfused with ice-cold 0.9% saline followed by 4% paraformaldehyde (PFA) in 0.1 M phosphate buffer (PB). Brains were excised, fixed overnight in 4% PFA in 0.1 M PB, and either embedded in 2.5% agarose and sectioned at 50 μm by vibratome (Leica) or cryoprotected with 30% sucrose in PB at 4°C overnight, embedded, and frozen in OCT (TissueTEK), and 30 μm floating sections cut by cryostat (Leica). For whole-mount immunostaining of the V-SVZ, brains of mice were excised and fixed overnight in 4% PFA in 0.1 M PB, washed in PBS followed by microdissection under a binocular, and immunostained as previously described [13].

Immunofluorescence Staining of Floating Sections and Antibodies

Immunostaining on sections was performed essentially as described previously [6, 21]. Briefly, sections were blocked at room temperature for 30 minutes with 2% normal donkey serum or 5% normal goat serum (Jackson Immunoresearch, West Grove, PA, http://www.jacksonimmuno.com) in phosphate buffered saline (PBS) containing 0.5% Triton X-100. Primary antibodies diluted in blocking solution were incubated overnight at 4°C. Sections were washed with PBS and incubated at room temperature for 1–2 hours with the corresponding secondary antibodies and counter-stained with DAPI (1 μg/mL). For signal amplification, sections were washed and incubated for 1 hour in streptavidin conjugated to fluorescein isothiocyanate (FITC) or Cy3. Sections were mounted on glass slides (SuperFrost, Menzel) in DABCO mounting media and visualized using a Zeiss LSM510 confocal microscope (Zeiss, Jena, Germany, http://www.zeiss.com). For BrdU detection, sections were treated prior to the blocking step with 2 N HCl at 37°C for 30 minutes. For proliferating cell nuclear antigen (PCNA) detection, the antigen was recovered at 80°C for 20 minutes in sodium citrate (10 mM, pH 7.4). Antibodies and streptavidin conjugates used were as follows: anti-BrdU (rat, 1:2,000, Serotec, Oxford, U.K., http://www.serotec.com), anti-Ascl1 (Mouse, 1:200, BD Pharmingen, San Diego, CA, http://www.bdbiosciences.com/

index[lowen]us.shtml), anti-β-catenin (mouse, 1:100, BD Trans labs), anti-β-tubulinIII (mouse, 1:500, Sigma), anti-BLBP (rabbit, 1:1500, Chemicon, Temecula, CA, http://www.chemicon.com), anti-Calbindin D28k (rabbit, 1:500, Swant), anti-calretinin (rabbit, 1:500, Swant), anti-CD31 (rat, 1:500, BD Pharmingen), anti-Cre recombinase (rabbit, 1:1,000, Novagen), anti-Cre recombinase (mouse, 1:1,000, Nordic Biosite), anti-doublecortin (goat, 1:5,000, Santa Cruz Biotechnology Inc., Santa Cruz, CA, http://www.scbt.com), anti-GFAP (mouse, 1:500, Sigma), anti-GFAP (rabbit, 1:1,000, Sigma), anti-green fluorescent protein (GFP) (sheep, 1:500, Biogenesis), anti-GFP (rabbit, 1:500, Invitrogen), anti-GFP (chicken, 1:500, AvesLabs), anti-Musashi1 (rat, 1:500, gift from H. Okano), anti-nestin (mouse, 1:500, Chemicon), antineuronal nuclear antigen (mouse, 1:500, Sigma), anti-O4 (mouse, 1:50, gift from M. Schwab), anti-PCNA (mouse 1:1,000, DAKO, Glostrup, Denmark, http://www.dako.com), anti-S100β (rabbit, 1:500, Swant), anti-Sox2 (rabbit, 1:500, Chemicon), anti-tyrosine hydroxylase (mouse, 1:1,000, Chemicon). Secondary antibodies and detection: FITC/Cy3/Cy5-conjugated anti-mouse, rabbit, rat, and guinea pig immunoglobulin, and biotinylated anti-sheep, and anti-donkey immunoglobulin (1:500, Jackson Immunoresearch), Alexa488-conjugated streptavidin (1:2,000, Molecular Probes, Eugene, OR, http://probes.invitrogen.com), and FITC-conjugated streptavidin (1:400, Jackson Immunoresearch).

Cell Isolation for Fluorescence-Activated Cell Sorting, EGF binding, Neurosphere Assays, and In Vitro Differentiation

Brains of adult mice were sectioned at 300 μm using a McIll-wains tissue chopper in ice-cold L15 medium (Gibco, Invitrogen, Grand Island, NY, http://www.invitrogen.com). The V-SVZ was microdissected under a binocular microscope. Tissue was digested with a papain-based solution and mechanically dissociated as described previously [20]. Cells were washed with L15 medium (Gibco, Invitrogen), filtered through a 30-μm cell sieve, and sorted by forward/side-scatter and gated for GFP^{-}/ $mCherry^{-}$ or positive populations. To label the EGF-binding cell populations, cells were incubated for 30 minutes with bio-tinylated EGF complexed with Alexa647-streptavidin (2 μg/mL; Molecular Probes) prior to sorting as described previously [12]. Cells were plated at clonal density (0.1 cell per μL) in 96-well plates in neurosphere medium containing Dulbecco's modified Eagle's medium (DMEM):F12 (Gibco, Invitrogen), B27 (Gibco, Invitrogen), EGF 10 ng/mL (R&D Systems, Minneapolis, MN, http://www.rndsystems.com). Cultures were fed at day 3. Neurosphere number was counted at day 6. Six to twelve independent samples and 8–48 wells per sample were used per condition. Clones were established from adult mice. Single cells were isolated as above and plated by preparative fluorescence-activated cell sorting (FACS) (FACSCaliburs, Becton Dickinson, Franklin Lakes, NJ, http://www.bd.com) in wells containing neurosphere culture medium. Clones of *Hes5::GFP*$^{+}$ and *BLBP::mCherry*$^{+}$ cells were passaged five to six times and plated as neurospheres onto poly-L-lysine and laminin-coated dishes in differentiation medium containing DMEM:F12 and B27 and cultured for 14 days. Cells were fixed 10 minutes in 4% PFA and processed for immunostaining as described above.

Generation of Ad:GFAP-Cre Virus

Generation of Ad:GFAP-Cre virus was described previously [28]. Briefly, Cre was placed under the control of the mouse GFAP promoter (GFAPp) previously confirmed to be specifically active in $GFAP^+$ cells. The pAd/PLGFAPp-NLSCre-pA vector was transfected into HEK293 cells to produce replication-defective adeno-virus, which was purified twice by cesium chloride banding. The titer was 1×10^{12} infectious particles per milliliter.

EGF or Ad:GFAP-Cre Virus Infusions into the Lateral Ventricles

Adult (2–3 months old) *Hes5::GFP* mice were anesthetized by i.p. injection of a ketamine/xylazine solution (100 mg and 5 mg/ kg b.wt., respectively) and positioned in a stereotaxic apparatus (David Kopf instruments) [6]. The skull was exposed by an incision in the scalp and a small hole (1 mm) drilled through the skull. Human recombinant EGF (R&D Systems, 33 ng/μL in saline, 0.1% bovine serum albumin) or vehicle alone was infused into the lateral ventricle for 6 days with an osmotic-pump according to manufacturer's instructions (Alzet, model 1007D. 396 ng EGF per day). Cannulas (Alzet, Brain infusion kit 3) were implanted at 0 mm anteroposterior, 1 mm lateral to bregma, and 2.5 mm below the surface of the skull [29]. After 6 days of infusion, animals received a single i.p. BrdU injection (50 mg/kg b.wt.) and were sacrificed 2 hours later. One microliter of Ad:GFAP-Cre virus (titer 1×10^{12} infection particles per mL) was injected into the lateral ventricle of 2-month-old *Rosa-CAG::GFP* mice using sharpened Borosilicate glass capillaries (Kwick-Fil) and the following stereotaxic coordinates: at 0 mm anteroposterior, 1 mm lateral to bregma, and 2.5 mm below the surface of the skull. Mice were killed 3 or 14 days after virus injection. Brain tissue was processed and analyzed by immunohistochemistry as described above.

Early Postnatal Electroporation and Lineage Tracing of $BLBP^+$ Cells

Inducible genetic lineage tracing of $BLBP^+$ cells was performed by electroporation of *BLBP::CreER*^{T2} and *BLBP::mCherry* constructs into the V-SVZ of *Rosa-CAG::GFP* transgenic mice, followed by TAM induction and analysis of cells where the *Rosa-CAG::GFP* Cre-reporter allele had been recombined resulting in constitutive expression of eGFP (referred to as rGFP). For the injection of DNA constructs, a microinjector (Pneumatic Pico Pump, WPI Rnage) and pulled, sharpened Borosilicate glass capillaries (Kwick-Fil) were used. The capillaries were back-loaded with 10 μL of endotoxin-free plasmid in sterile PBS at a concentration of 1.5 μg/μL. Fast green contrast dye (10%) was added to the plasmids to visualize the targeted area of the telencephalon. Postnatal day 1–2 (P1–2) *Rosa-CAG::GFP* transgenic mice were anesthetized by hypothermia on ice. A cold light source was used to illuminate the pups during the procedure. Two microliters of DNA solution (3 μg) were injected into the right lateral ventricle of each mouse pup. The pups were electroporated (Electro Square Pavator, BTX Harvard Apparatus) with five pulses of 100 mV and a pulse length of 50 ms at 950 ms intervals. The anode of the electrode was oriented lateral to the right hemisphere. After electroporation, the pups were warmed under a lamp while being monitored until they could be returned to the mother. 20 days after electroporation (P21–22) mice were injected daily i.p. with 2 mg TAM in corn oil (100 μL of 20 mg/mL) for five consecutive days and sacrificed 1 or 45 days after the end of the TAM treatment. BrdU (0.8 mg/mL in the drinking water) was administered to the mice of the 45

days chase experiment during the last 7 days before killing. Brain tissue was processed for immunohistochemistry as described above.

Quantification and Statistical Analysis

Stained cells were analyzed with fixed photomultiplier settings on a Zeiss LSM510 confocal microscope (Zeiss). Data are presented as average percentages of colabeled cells. The number of marker-positive cells in the V-SVZ was estimated using a × 63 magnification objective and confocal Z-sectioning followed by 3D reconstruction. For quantification of GFAP expression, confocal 3D reconstructions of the entire cell body and processes of SVZ cells were obtained from 30 μm thick coronal sections. A cell was considered GFAP$^+$ if GFAP expression was detected in at least one process. Cytoplasmic proteins that also localized to the processes of cells such as GFP from the *Hes5::GFP* locus, BLBP, mCherry from the *BLBP::mCherry* locus, or rGFP from the recombined *Rosa-CAG::GFP* locus were used to visualize cellular processes in their entirety. The DAPI-stained area of the V-SVZ was measured with ImageJ software and used to estimate the number of labeled cells per mm^2. The Shapiro-Wilk test was applied to assess for normal distribution of the data. Statistical comparisons were conducted by two-tailed unpaired Student's *t* test. Significance was established at $p < 0.05$. In all graphs, the error bars are SD unless otherwise stated. Data tables are presented in Supplementary Information.

Human Brain Tissue Samples

Brain tissue (prenatal 21 weeks, $n = 1$; postnatal 14–27 months, $n = 4$) was obtained from the Institute of Pathology, University Hospitals of Basel, during routine postmortem neuropathological examination with authorization by the local Ethics Committee. Tissue blocks were routinely processed and paraffin embedded, serially sectioned at 3 μm, and immuno-stained as described [30].

Results

Genetic Lineage Tracing Reveals Heterogeneity in V-SVZ NSCs

The SVZ of adult mice contains GFAP$^+$ B1 cells that extend apical processes into V-SVZ. We lineage traced *GFAP::CreER^{T2}* expressing cells in adult mice by monitoring recombination of a *Rosa26::YFP* Cre-reporter allele and examined how homogeneous B1 cells are in the adult V-SVZ (Fig. 1A). Twenty-four hours after 5 days of TAM treatment to induce Creactivity, most labeled cells (rYFP) expressed GFAP protein (Fig. 1B–1F). 25% of the rYFP$^+$ cells in the V-SVZ expressed both GFAP and BLBP indicating heterogeneity in the GFAP$^+$ population. A few YFP$^+$cells expressed BLBP but not GFAP and the others included TAPs and neuroblasts (Fig. 1F). After a 10-day chase period, the proportion of GFAP$^+$ cells among the rYFP$^+$ cells decreased consistent with the generation of increased numbers of more differentiated progeny. However, the fraction of BLBP$^+$GFAP$^+$ cells among rYFP$^+$GFAP$^+$ cells remained relatively constant and the rYFP$^+$BLBP$^+$GFAP$^-$ population increased suggesting that some of these were either generated or expanded during the chase period (Fig. 1F). In a complementary approach, we used an adenovirus-expressing Crerecombinase under the control of the *Gfap* promoter which we injected into the lateral ventricle of adult mice to infect V-SVZ cells (Fig. 1G–1M). Three days after

infection, the phenotype of the rGFP (*Rosa-CAG::GFP* reporter) labeled cells reflected that seen with the *GFAP::CreER^{T2}* transgenic approach with few labeled differentiated progeny (TAPs and neuroblasts) but a significant population of rGFP$^+$BLBP$^+$GFAP$^+$ cells. These rGFP$^+$BLBP$^+$GFAP$^+$ cells remained over the next 10 days as the number of newly generated neuroblast migrating in the RMS increased (Fig. 1K–1M).

BLBP Is Expressed by *Hes5*$^+$ Cells in the V-SVZ

V-SVZ NSCs depend on canonical Notch signaling for their maintenance and quiescence [7, 23]. We addressed whether BLBP$^+$ cells displayed Notch signaling. *Hes5::GFP* reports canonical Notch signaling and all *Hes5::GFP*$^+$ (referred to as *Hes5*$^+$) cells in the SVZ and V-SVZ expressed Sox2 and Musa-shi1 but not the TAP (C cell) associated transcription factor Ascl1, the neuroblast protein Dcx or S100β (postmitotic astrocytes and ependymal cells) (Supporting Information Fig. S1A–S1F) [7, 16, 21, 25]. However, *Hes5*$^+$ cells in the V-SVZ were heterogeneous, and included GFAP$^+$ cells, some of which also expressed BLBP, and others that expressed BLBP but not detectable levels of GFAP protein even in their processes (Fig. 2A–2E). In addition, a fraction of the *Hes5*$^+$ cells were proliferating (PCNA$^+$; Supporting Information Fig. S1E).

Hes5$^+$ cells were an integral part of pinwheel structures consistent with being stem cells (B1 cells) and were surrounded by ependymal cells which do not express *Hes5::GFP* (Fig. 2F; Supporting Information Fig. S1D). Pinwheels included *Hes5*$^+$BLBP$^+$ and *Hes5*$^+$BLBP$^-$ cells supporting heterogeneity in this stem cell population (Fig. 2F). 3D analysis of ventricular en face views of the SVZ revealed individual pinwheels that contained both GFAP$^+$ and BLBP$^+$ B1 cells (Fig. 2G). Consistent with being progenitors, *Hes5*$^+$ cells were a small population in the adult V-SVZ and sorting *Hes5*$^+$ cells enriched for multipotent neurosphere-forming potential (Supporting Information Fig. S1G–S1I).

Hes5$^+$ Cells Include V-SVZ NSCs

We used *Hes5::CreER^{T2}* transgenic mice to perform genetic lineage tracing and assess the potential of *Hes5*$^+$ cells in vivo (Supporting Information Fig. S1J) [25]. *Hes5::GFP* and *Hes5::CreER^{T2}* expression overlapped (95.9% ± 0.98%) in double-transgenic mice indicating labeling of the same population. Cremediated recombination of the *Rosa-CAG::GFP* allele resulted in constitutive expression of eGFP (rGFP) by *Hes5::CreER^{T2}* cells and their progeny (Supporting Information Fig. S1K) [25]. One day after the TAM induction (d1), rGFP$^+$ cells in the V-SVZ expressed *Hes5::CreER^{T2}* and GFAP and/or BLBP (Supporting Information Fig. S1L–S1N). rGFP$^+$ neuro-blasts and neurons were not present in the RMS or OB at this time (Supporting Information Fig. S1O). Twenty-one days after TAM induction (d21), many rGFP$^+$ neuroblasts were present in the SVZ, along the RMS and in the OB indicating neuron production by *Hes5::CreER^{T2}* cells (Supporting Information Fig. S1P, S1Q). 100 days after TAM induction, rGFP$^+$ cells in the V-SVZ continued to generate mitotic progenitors (PCNA$^+$) and neuroblasts in the V-SVZ and RMS confirming that the targeted NSCs retain long-term neurogenic potential (Supporting Information Fig. S1R). rGFP$^+$ cells reached the OB over time and newly formed neuroblasts migrated to the granule and periglomerular layers and differentiated into neurons

(Supporting Information Fig. S1S–S1V). Thus, *Hes5*$^+$ cells include NSCs in the V-SVZ and remain in the niche over months while continually generating neurons [31–34].

BLBP Expression Subdivides the *Hes5*$^+$ NSC Population

Intrigued by the heterogeneity in the GFAP and *Hes5*$^+$ populations, we examined *Hes5*$^+$ cells in the V-SVZ in greater detail. *Hes5*$^+$BLBP$^+$ cells did not express Ascl1 but were associated with Ascl1$^+$ TAPs thereby distinguishing them as a separate population (Fig. 2H, 2I). We identified three types of *Hes5*$^+$ B1 cell which included GFAP$^+$BLBP$^-$, GFAP$^+$BLBP$^+$, and GFAP$^-$BLBP$^+$ cells of approximately equal numbers in the V-SVZ and defined these as type 1, 2, and 3 NSCs (Fig. 2E, 2J). Interestingly, BLBP expression also seemed to subdivide the Ascl1$^+$ TAP cells into two populations (potentially early and late) implying that BLBP is expressed by active NSCs and early TAPs while being expressed at lower levels in more mature late Ascl1$^+$ cells (Fig. 2I, 2J).

BLBP$^+$ Progenitors Include Neurogenic NSCs

We examined BLBP$^+$ cells in the V-SVZ by genetic lineage tracing using the *Rosa-CAG::GFP* Cre-reporter. We concentrated on resident V-SVZ cells rather than transient populations by electroporating progenitors in the lateral ventricle walls of postnatal mice with *Blbp::CreER*^{T2} and *Blbp::mCherry* constructs but only induced lineage tracing 20 days later with a 5-day TAM treatment (Fig. 3A, 3B). The 20-day chase phase before TAM treatment circumvented labeling BLBP expressing TAPs. We hypothesized that any TAPs that were initially trans-fected would differentiate and migrate out of the SVZ during this chase period. Hence, cells labeled in the SVZ following this protocol are resident BLBP-expressing SVZ cells. Confirming this, rGFP$^+$ cells in the V-SVZ expressed BLBP (mCherry) 1 day after Cre-induction (Fig. 3C) and included GFAP$^+$ (type 2) as well as GFAP$^-$ (type 3) radial B1 cells (Fig. 3C–3E; Supporting Information Fig. S2A–S2D). Many rGFP$^+$ cells were detected in the OB 45 days postinduction but not 1 day after TAM treatment (Fig. 3F). The density of rGFP$^+$ cells derived from *BLBP::CreER*^{T2} expressing cells in the V-SVZ increased between day 1 and day 45 after induction both in the SVZ and OB consistent with amplification and generation of multiple progeny (Fig. 3G). *BLBP::CreER*^{T2}-derived cells (rGFP$^+$) in the OB were neuroblasts and neurons (Fig. 3H–3J). We examined whether *BLBP::CreER*^{T2} cells remained in the SVZ and continued to proliferate and generate new neuroblasts (Dcx$^+$) which would be consistent with being stem cells rather than short-lived TAPs. We pulsed mice for the last 7 days of the 45-day chase with BrdU and found that *BLBP::CreER*^{T2}-derived cells continued to generate mitotic progenitors and neuroblast (Fig. 3K, 3L). The majority of the rGFP$^+$ cells at day 1 expressed BLBP but most were BLBP$^-$ progeny by day 45 (Fig. 3M). Thus, BLBP$^+$ V-SVZ cells included a long-term neurogenic population that generated increasing numbers of progeny with time.

BLBP Expression by *Hes5*$^+$ Cells Correlates with EGFR Expression and Neurospherogenic Potential in the V-SVZ

We generated mice expressing the red fluorescent protein mCherry under the control of the regulatory elements of the *Blbp* gene (*Blbp::mCherry*) to study *Hes5*$^+$BLBP$^+$ NSCs in

greater detail (Fig. 4A). In agreement with our findings for BLBP protein, a subpopulation of *Hes5*$^+$ cells expressed *Blbp::mCherry* (Supporting Information Fig. S3A, S3B) and these also expressed BLBP protein (Fig. 4B). *Blbp::mCherry*$^+$*Hes5*$^-$ cells expressed Ascl1, suggesting they were TAPs (Supporting Information Fig. S3C and data not shown). EGF-dependent V-SVZ neurospheres are generated by activated stem/progenitor cells [12, 35, 36]. We sorted *Hes5::GFP* and *Blbp::mCherry* double-positive cells and analyzed the GFP$^+$ (*Hes5*) and mCherry$^+$ (*Blbp*) populations in neurosphere assays (Fig. 4C). *Hes5*$^-$*Blbp*$^-$ cells did not form neurospheres and *Hes5*$^+$*Blbp*$^+$ cells generated neurospheres more efficiently than the *Hes5*$^+$*Blbp*$^-$ and *Hes5*$^-$*Blbp*$^+$ cells (Fig. 4D). *Hes5*$^+$*Blbp*$^+$, *Hes5*$^+$*Blbp*$^-$ and *Hes5*$^-$*Blbp*$^+$ cells were expandable as multipotent neurospheres indicating self-renewal of NSC (*Hes5*$^+$) and TAP (*Hes5*$^-$*Blbp*$^+$) populations in vitro (Supporting Information Fig. S3D, S3E). The high neurospherogenic potential among *Hes5*$^+$BLBP$^+$ cells supports the interpretation that neurospheres in the V-SVZ are predominantly derived from the activated NSCs and that this population expresses *Hes5* and BLBP.

We reanalyzed the expanded cultures derived from GFP, mCherry, and double-positive cells for GFP and mCherry expression by dissociation of clonal neurosphere cultures and FACS analysis. Many cells in the *Hes5*$^+$-derived clonal cultures retained GFP expression (41% ±21%, *n* =6). A few *Hes5*$^-$*Blbp*$^+$ cells activated *Hes5::GFP* expression (GFP$^-$ became GFP$^+$) in culture (10% ±8% *n* =6) implying a conversion to a more stem cell-like character. All neurosphere cultures derived from *Blbp::mCherry*$^+$ cells retained mCherry expression, irrespective of *Hes5::GFP* expression by their founder cell (99% ±3%, *n* =4). Interestingly, many *Hes5*$^+$*Blbp*$^-$ cells activated *Blbp::mCherry* expression in culture (53% ±33%, *n* =5) proposing that *Hes5*$^+$*Blbp*$^-$ NSCs can generate *Blbp*$^+$ neurospherogenic cells in vitro. Therefore, *Hes5*$^+$BLBP$^+$ NSCs retained BLBP expression but also generated *Hes5*$^-$ putative TAP neurospheres in vitro. Conversely, some *Hes5*$^+$*Blbp*$^-$ NSCs generated *Blbp*$^+$ neurospheres, however, we never observed *Hes5*$^+$*Blbp*$^+$ cells becoming *Hes5*$^+$*Blbp*$^-$ which is consistent with NSCs in vitro remaining in an active state likely due to the high levels of mitogen.

In order to better characterize this neurosphere-forming population, we investigated if the EGFR was expressed (via EGF binding and FACS [12]) by *Hes5*$^+$ and *Blbp*$^+$ cells in the V-SVZ. By quantitative FACS analysis, 28.0% ±10.5% of the *Hes5*$^+$ NSCs expressed EGFR (Fig. 4E). 92.4 % ±7.4% of the *Hes5*$^+$BLBP$^+$ cells expressed EGFR but only 13.8% ±3.8% of the *Hes5*$^+$BLBP$^-$ cells bound EGF (Fig. 4E). Most *Hes5*$^-$ BLBP$^+$ TAPs expressed EGFR (79.0% ±7.49%; Fig. 4E). Hence, overlap of Hes5, BLBP, and EGFR in the V-SVZ labels a major neurospherogenic population of putative activated progenitors that do not express TAP markers and are likely NSCs.

Hes5$^+$ BLBP$^+$ NSCs Expand In Vivo in Response to EGF

Multiple growth factors can influence proliferation in the V-SVZ and adult forebrain neurogenesis [37]. We investigated the responses of *Hes5*$^+$BLBP$^+$ cells to EGF in vivo by infusion into the forebrain ventricles for 6 days (Fig. 4F) [36]. EGF infusion resulted in expansion of the V-SVZ and increased cell proliferation including an increased BrdU incorporation (2 hours after injection) by *Hes5*$^+$ cells (Fig. 4G, 4H). The number of

Hes5$^+$BLBP$^+$ cells were increased slightly by EGF treatment compared to the saline infused controls while the *Hes5*$^+$GFAP$^+$ population was reduced (Fig. 4I, 4J and not shown). Interestingly, all proliferating *Hes5*$^+$ cells expressed BLBP after EGF treatment (not shown).

Hes5$^+$ BLBP$^+$ NSCs Are Mitotically Active

It has been suggested that the majority of the NSCs in the V-SVZ are quiescent, but an actively dividing subpopulation with a relatively short cell cycle have recently been described [38]. We analyzed the proliferative characteristics of the various *Hes5*$^+$ populations in the V-SVZ. Most *Hes5*$^+$ NSCs were PCNA$^-$ and thus mitotically inactive consistent with being quiescent NSCs (92% ±1.4%; Fig. 5B). Although they express progenitor markers including Sox2, it remains unclear whether all *Hes5*$^+$PCNA$^-$ cells are primary progenitors or some may be dormant NSCs or postmitotic astrocytes. *Hes5*$^+$PCNA$^+$ cells were a minor proportion of the total proliferating cell population in the V-SVZ (8.5% ±1.9%; Fig. 5B), and most *Hes5*$^+$PCNA$^+$ cells expressed BLBP (73.6% ±11.6%; Fig. 5C). Similarly, most *Hes5*$^+$BrdU$^+$ cells expressed BLBP protein following a 2-hour BrdU pulse and were a minor fraction of both the *Hes5*$^+$ and the total BrdU$^+$ populations in the V-SVZ (Fig. 5A–5C).

After a 15-day cumulative BrdU label, the proportion of *Hes5*$^+$ cells that incorporated BrdU increased from 2.0% ±1.3% to 8.7% ±0.7% of the total *Hes5*$^+$ cell population, comparable to the proportion of *Hes5*$^+$ cells that are in the cell cycle at any point in time (PCNA$^+$−8.0% ±1.4%) (Fig. 5D, 5E). Most *Hes5*$^+$BrdU$^+$ cells expressed BLBP but no longer expressed PCNA indicating they had passed through S-phase and subsequently exited cell cycle to become quiescent (Fig. 5E). We performed BrdU retention assays giving a 30-day chase period after 15 days of cumulative BrdU labeling (d45). The percentage of *Hes5*$^+$ cells labeled with BrdU$^+$ remained constant between day 15 and day 45 and most expressed BLBP protein. We inferred that this population had entered a quiescent state (Fig. 5E). These findings indicate that *Hes5*$^+$BLBP$^+$ cells divide infrequently probably by exiting the cell cycle and thus retain S-phase label. As most of the label-retaining *Hes5*$^+$ cells expressed BLBP but did not express GFAP, *Hes5*$^+$ cells that exit cell cycle do not become type 1 NSCs or differentiate into postmitotic SVZ astrocytes but remain or become type 2/3 NSCs. Therefore, BLBP expression by *Hes5*$^+$ cells correlates with both mitotic activity and label retention (Fig. 5E). *Hes5*$^+$GFAP$^+$ cells that were in the cell cycle (PCNA$^+$), or incorporated BrdU, or were label retaining, were always far fewer than those that expressed *Hes5* and BLBP indicating that GFAP$^+$ NSCs are less proliferative than BLBP$^+$ NSCs (Fig. 5C, 5E).

Active *Hes5*$^+$ BLBP$^+$ Cells Dramatically Reduce with Age

Neurogenesis in the murine V-SVZ declines with age. Whether NSCs are lost or their mitotic activity diminishes remains unclear [39]. We addressed whether *Hes5*$^+$ NSC subpopulations are differentially affected during aging. The total number of *Hes5::GFP*$^+$ NSCs was reduced in the V-SVZ of aged compared to young mice (Supporting Information Fig. S4A–S4D). This was mirrored by a significant decrease in *Hes5*$^+$BLBP$^+$ NSCs (type 2 and type 3) and a dramatic reduction in proliferating cells (PCNA$^+$ cells) in the V-SVZ of aged mice (Supporting Information Fig. S4A–S4D). By contrast, *Hes5*$^+$GFAP$^+$ NSCs (mainly type 1) were not significantly affected by age (p =.13; Supporting Information Fig.

S4C, S4D). *Hes5*$^+$ NSCs that remained in the aged brain proliferated less than their younger counterparts indicating an imbalance of the quiescent versus active NSC fractions or an increase in the terminal differentiation of primary progenitors (Supporting Information Fig. S4E). This suggested a shift of NSCs to a quiescent/dormant state and a loss of the more mitotically active *Hes5*$^+$ type 2 and type 3 NSCs. Thus, a decrease in *Hes5*$^+$BLBP$^+$ active cells coincided with the reduced proliferation in old mice suggesting that the specific loss of active BLBP$^+$ NSCs might underlie the age-related decline in neurogenesis.

BLBP Expression Correlates with Mitotic Activity in the Human VZ and V-SVZ

Radial glial progenitors in the VZ and outer SVZ of the developing brain generate neurons also in humans [40]. We examined the expression of BLBP by VZ progenitors in the 21 week fetal human forebrain (Fig. 6A–6D). VZ cells in humans (likely radial glia), like in mice, expressed BLBP and were mitotically active. Many proliferative cells (Ki67 or PCNA$^+$) in the VZ expressed BLBP and many also expressed GFAP (Fig. 6B–6D). Dividing cells in the SVZ that likely represented committed intermediate progenitors did not express BLBP. Neurogenesis in the lateral walls of the human forebrain ventricles diminishes rapidly during the first 3 years after birth and this is associated with the formation of an astrocytic ribbon and a hypocellular gap next to the VZ (Fig. 6E) [41]. Interestingly, we observed that a subpopulation of cells in the astrocytic ribbon in a 14-month-old infant brain were BLBP$^+$ (Fig. 6F). Consistent with the previously reported reduction in proliferation, we observed few proliferating cells in the 14-month old infant SVZ. Interestingly some of the cells that continue to proliferate (Ki67$^+$) also expressed BLBP (Fig. 6G–6I) [41]. Some of these BLBP$^+$ cells within the astrocytic ribbon showed a radial morphology (Fig. 6I).

Discussion

The V-SVZ is the major neurogenic region in the forebrain of postnatal mammals contributing thousands of neurons to the OB and prefrontal cortex in infant humans [41]. However, characterization of NSCs has proven challenging and particularly the identification of activated NSCs in the adult V-SVZ has been elusive. Although NSCs are perceived as a homogeneous population of multipotent primary progenitors, they are fate-restricted based on their developmentally determined position within the V-SVZ and therefore more heterogeneous than anticipated [10, 28].

Neurogenic NSCs in the V-SVZ depend on Notch signaling [7, 23]. Here we provide multiple lines of evidence for heterogeneity within the NSC population and uncover active BLBP$^+$ NSC types that are part of the center pinwheel structures where B1 cells have apical contacts with the lateral ventricle wall. Our results indicate that *Hes5*$^+$BLBP$^+$ type 2 and type 3 NSCs are long-term neurogenic stem cells that self-renew in vivo. By contrast, *Hes*$^+$BLBP$^-$ type 1 NSCs are mostly quiescent in vivo and in agreement form less colonies than *Hes5*$^+$BLBP$^+$ NSCs (type 2 and type 3) in vitro. This suggests that active neurogenic stem cells in the adult forebrain express BLBP and thereby retain a similar antigenic signature to radial glial cells during development [42, 43].

Hes5$^+$ BLBP$^+$ NSCs are not a transient population as they do not express TAP markers, they enter and exit the cell cycle, retain S-phase label and express stem cell markers, and can

remain neurogenic for months in the V-SVZ. Thus, BLBP$^+$ cells are a major S-phase label-retaining population with active Notch signaling in the V-SVZ. Our BrdU label retention, *BLBP::CreER^{T2}* and *GFAP::CreER^{T2}* lineage tracing data suggest that activated BLBP$^+$ cells that exit the cell cycle and remain in the V-SVZ do not upregulate GFAP and are replaced by quiescent BLBP$^+$ type 2 and type 3 NSCs that become activated rather than BLBP$^-$ type 1 NSCs. Thus, under physiological conditions, BLBP$^+$ NSCs do not readily convert into BLBP$^-$GFAP$^+$ NSCs in vivo (Fig. 7). We cannot exclude that type 1 NSCs give rise to BLBP$^+$ NSCs at a very low rate or under pathological situations such as injury. Indeed, we found that BLBP$^-$ type 1 NSCs can upregulate BLBP in vitro implying that GFAP$^+$BLBP$^-$ NSCs may be more primitive or a reserve pool to generate activated NSCs. A caveat with the analysis of stem cell identity and fate is that the current transgenic tools and markers are not able to address the lineage relationship between type 1, 2, and 3 NSCs in vivo.

Lineage tracing studies assume stable reporter gene expression in each cell type. Embryonic neural progenitors show dynamic gene expression [44]. Although a similar dynamic gene expression has not been shown for adult NSC subpopulations and this may affect the interpretation of lineage tracing experiments, we do not have evidence for dynamic changes in GFAP or *Blbp* expression during the cell cycle of *Hes5*$^+$ NSCs. We detected similar numbers of *Hes5*$^+$BLBP$^+$GFAP$^-$ and *Hes5*$^+$BLBP$^+$GFAP$^+$ NSCs that were in the cell cycle (PCNA$^+$) or that incorporated S-phase label (2-hour BrdU pulse) or that retained the BrdU label and became quiescent (Fig. 5). Therefore, we propose that molecular diversity subdivides the adult NSC compartment into distinct populations with different proliferative dynamics rather than states of the same cell. However, the lack of cellular specificity of the current transgenes compounds these problems.

EGF activates V-SVZ progenitors directly and indirectly reversibly blocking their differentiation [9, 12, 29, 36]. Cells that are EGF responsive and that proliferate in vivo can form neurospheres [12, 35]. We found that the *Hes5*$^+$BLBP$^+$ NSC populations express EGF receptors and they are the major EGF-dependent neurospherogenic population with B1-cell characteristics in the V-SVZ. In addition, BLBP$^+$ NSCs proliferate in response to EGF infusion in vivo, contributing to the expansion of the V-SVZ and increase in BLBP$^+$ cells in the *Hes5*$^+$ NSC population. Based on the neurosphere formation ability of *Hes5*$^+$BLBP$^+$ cells and enrichment of EGFR expression in this NSC population, it is likely that EGF directly affects proliferation of BLBP$^+$ NSCs in vivo and we suggest that the increase in BLBP$^+$ NSCs upon EGF treatment is due to their symmetric self-renewal. However, we did observed an upregulation of *Blbp::mCherry* by *Hes5*$^+$*Blbp*$^-$ neurospheres in response to mitogen. Hence, our finding that a mitotically active *Hes5*$^+$BLBP$^+$ self-renewing population coexist with more quiescent NSCs is similar to findings in other somatic adult tissues and raises the possibility that not all V-SVZ NSCs are quiescent [21, 38, 45–47]. Complex genetic labeling with combined inducible Cre and Flpe transgenes will be required to attempt to address the relationship between type 1, 2, and 3 NSCs in vivo under physiological and pathological conditions.

Neurogenesis in the forebrains of mammals diminishes dramatically with age. A fundamental question that remains is whether the reduction in neurogenesis during aging

reflects depletion of NSCs or increased NSC quiescence [21, 48, 49]. This issue remains controversial as previous studies of the aged V-SVZ did not take into account NSC heterogeneity or the differential effects aging may have on NSC subtypes [50]. The V-SVZ niche in aged mice contains substantially reduced numbers of *Hes5*$^{+}$ NSCs. This implies that NSC depletion is a contributing factor in the impaired V-SVZ neurogenesis in aged mice. Importantly, BLBP^{+} and BLBP^{-} NSC subpopulations were differentially affected by aging. Although BLBP^{+} type 2 and type 3 NSCs were scarce in the V-SVZ of old mice and this paralleled the decreased size of the overall *Hes5*$^{+}$ population, many *Hes5*$^{+}$BLBP^{-} cells including GFAP^{+} type 1 NSCs remained. These remaining *Hes5*$^{+}$ NSCs in the aged V-SVZ divided less frequently than their young counterparts consistent with our findings that *Hes5*$^{+}$BLBP^{-} type 1 NSCs are mitotically less active than *Hes5*$^{+}$BLBP^{+} NSCs (Fig. 7). This suggests that increased quiescence is a second factor contributing to the decrease in neurogenesis in the aged V-SVZ, which is in agreement with previous studies [51] and reminiscent of *Hes5*$^{+}$ NSCs within the aged hippocampus [21]. It is possible that some active *Hes5*$^{+}$BLBP^{+} NSCs enter a dormant state, upregulate GFAP, and loose BLBP expression during aging. Understanding the mechanisms responsible for the age-related loss of active NSC in the mouse V-SVZ could help to understand why the majority of NSCs in the human brain stop generating neurons early during postnatal life [41]. We found that BLBP^{+} cells in the neurogenic zones of the developing and infant human brain can be mitotically active and their presence correlates with neuron production. This suggests that BLBP may be a potential marker for activated NSCs in humans and that active NSCs are lost or convert to astrocytes in the SVZ.

It will be important to determine the niche signals that control the proliferative and quiescent states toward activating potentially dormant NSCs in the adult and aged brain. Notch activity in the V-SVZ niche maintains NSCs and blocks neurogenesis and is thus a central regulator in the NSC niche [7, 23, 52]. How Notch signals control these multiple processes in NSCs remains to be clarified.

Why do active NSCs express BLBP? BLBP is a Notch target and a fatty acid binding protein implicated in lipid metabolism, transport, and signaling [53]. It is tempting to speculate that dividing cells have high energy requirements to support the rapid increase in cell mass and BLBP may play a role. Indeed, downregulation of BLBP (Fabp7) in rat neural progenitors reduces proliferation and *Fabp7*/*Fabp5* double knockout mice show aberrant neurogenesis in the hippocampus [54, 55]. This hypothesis is also indirectly supported by the expression of lipid metabolizing pathways in active progenitors in the brain opening up the possibility that lipid metabolism is differentially regulated in activated versus quiescent NSCs [56].

None of the NSC markers currently available exclusively label NSCs including Hes5 and BLBP. Hence, different studies rely on markers expressed in partially overlapping populations for lineage identification and tracing which could lead to different conclusions about cell identity. We performed side-by-side comparisons of populations of cells by combining multiple Cre lineage tracing approaches and fluorescent reporters with endogenous proteins. Through this comparative analysis we identified distinct subpopulations of NSCs in the adult V-SVZ, as well as their intersectional subpopulations,

and show that they behave differently in vivo and in vitro and during aging. Our analysis cannot exclude that NSCs switch between subtypes. We identify activated $BLBP^+$ NSCs in the adult V-SVZ that reside alongside more quiescent $BLBP^-$ stem cells thereby subdividing the NSC pool into three populations. The antigenic discrimination of $BLBP^-$ and $BLBP^+$ NSCs in the forebrain is intriguing, and it remains to be determined how the brain uses these NSC populations and their respective life spans under normal and pathological conditions. Cell-type-specific and combinatorial lineage tracing experiments need to be developed to assess these questions and fate map NSC as well as progenitor populations and their intersections simultaneously. In the light of recent data suggesting multiple NSC populations in the adult hippocampus and a potential glial differentiation of active hippocampal stem cells with age [21, 48, 57], it is important to address the lineage relationship between $GFAP^+$ and $BLBP^+$ NSCs during normal brain function and their responses in models of disease. Also the proportion of $GFAP^+$ cells that retain stem cell potential within the adult and aged SVZ needs to be functionally addressed. We present a model of stem cell heterogeneity in the adult V-SVZ placing the $BLBP^+$ NSC within the lineage of adult neurogenesis and a transition of NSCs to more quiescent states with age (Fig. 7). Therefore, we propose that the NSCs are potentially subdivided into three populations (type 1–3) based on antigenic profile and activity. Our results suggest that type 3 NSCs are produced by type 2 NSCs, the role and relationship with type 1 cells remains to be shown.

Conclusion

In summary, our data indicate that activated NSCs express BLBP and these are responsive to EGF. BLBP expressing NSCs divide more frequently than BLBP-negative B1 cells, hence, the SVZ NSC pool can be subdivided into three populations with distinct characteristics. It will be important to investigate the relationship between these three adult NSC populations under homeostatic and disease conditions and how the brain uses these different cells. Our data suggest that the presence of BLBP expressing NSCs in the mouse and human brain correlates with neurogenesis and that these cells are lost or enter a dormant state with age.

Supplementary Material

Refer to Web version on PubMed Central for supplementary material.

Acknowledgments

We thank the members of the Taylor lab for critical reading of the manuscript and for helpful discussions and Frank Sager for excellent technical assistance; Andy Wursch for help with the FACS. This work was supported by the Deutsche Forschungsge-meinschaft (SPP1109; TA-310) and by contract research “Adulte Stammzellen II” of the Baden-Wurttemberg Stiftung (P-BWS-ASII/ 29/30). O.B., S.L. and P.K. were former students of the faculty of Biology at the Albert Ludwigs University Freiburg. O.B. is currently affiliated with Hubrecht Institute, Uppsalalaan, CT Utrecht, The Netherlands; P.K. is currently affiliated with Friedrich Miescher Institute for Biomedical Research, Basel, Switzerland.

References

1. Morrison SJ, Spradling AC. Stem cells and niches: Mechanisms that promote stem cell maintenance throughout life. Cell. 2008; 132:598–611. [PubMed: 18295578]

2. Rossi DJ, Jamieson CH, Weissman IL. Stems cells and the pathways to aging and cancer. Cell. 2008; 132:681–696. [PubMed: 18295583]

3. Doetsch F. The glial identity of neural stem cells. Nat Neurosci. 2003; 6:1127–1134. [PubMed: 14583753]

4. Doetsch F, Garcia-Verdugo JM, Alvarez-Buylla A. Regeneration of a germinal layer in the adult mammalian brain. Proc Natl Acad Sci USA. 1999; 96:11619–11624. [PubMed: 10500226]

5. Ahn S, Joyner AL. In vivo analysis of quiescent adult neural stem cells responding to Sonic hedgehog. Nature. 2005; 437:894–897. [PubMed: 16208373]

6. Giachino C, Taylor V. Lineage analysis of quiescent regenerative stem cells in the adult brain by genetic labelling reveals spatially restricted neurogenic niches in the olfactory bulb. Eur J Neurosci. 2009; 30:9–24. [PubMed: 19558606]

7. Imayoshi I, Sakamoto M, Yamaguchi M, et al. Essential roles of Notch signaling in maintenance of neural stem cells in developing and adult brains. J Neurosci. 2010; 30:3489–3498. [PubMed: 20203209]

8. Fuentealba LC, Obernier K, Alvarez-Buylla A. Adult neural stem cells bridge their niche. Cell Stem Cell. 2012; 10:698–708. [PubMed: 22704510]

9. Ihrie RA, Alvarez-Buylla A. Lake-front property: A unique germinal niche by the lateral ventricles of the adult brain. Neuron. 2011; 70:674–686. [PubMed: 21609824]

10. Beckervordersandforth R, Tripathi P, Ninkovic J, et al. In vivo fate mapping and expression analysis reveals molecular hallmarks of prospectively isolated adult neural stem cells. Cell Stem Cell. 2010; 7:744–758. [PubMed: 21112568]

11. Ferron SR, Charalambous M, Radford E, et al. Postnatal loss of Dlk1 imprinting in stem cells and niche astrocytes regulates neurogenesis. Nature. 2011; 475:381–385. [PubMed: 21776083]

12. Pastrana E, Cheng LC, Doetsch F. Simultaneous prospective purification of adult sub-ventricular zone neural stem cells and their progeny. Proc Natl Acad Sci USA. 2009; 106:6387–6392. [PubMed: 19332781]

13. Mirzadeh Z, Merkle FT, Soriano-Navarro M, et al. Neural stem cells confer unique pinwheel architecture to the ventricular surface in neurogenic regions of the adult brain. Cell Stem Cell. 2008; 3:265–278. [PubMed: 18786414]

14. Artavanis-Tsakonas S, Rand MD, Lake RJ. Notch signaling: Cell fate control and signal integration in development. Science. 1999; 284:770–776. [PubMed: 10221902]

15. Louvi A, Artavanis-Tsakonas S. Notch signalling in vertebrate neural development. Nat Rev Neurosci. 2006; 7:93–102. [PubMed: 16429119]

16. Basak O, Taylor V. Identification of self-replicating multipotent progenitors in the embryonic nervous system by high Notch activity and Hes5 expression. Eur J Neurosci. 2007; 25:1006–1022. [PubMed: 17331197]

17. Mizutani K, Yoon K, Dang L, et al. Differential Notch signalling distinguishes neural stem cells from intermediate progenitors. Nature. 2007; 449:351–355. [PubMed: 17721509]

18. Pierfelice T, Alberi L, Gaiano N. Notch in the vertebrate nervous system: An old dog with new tricks. Neuron. 2011; 69:840–855. [PubMed: 21382546]

19. Aguirre A, Rubio ME, Gallo V. Notch and EGFR pathway interaction regulates neural stem cell number and self-renewal. Nature. 2010; 467:323–327. [PubMed: 20844536]

20. Nyfeler Y, Kirch RD, Mantei N, et al. Jagged1 signals in the postnatal subventricular zone are required for neural stem cell self-renewal. EMBO J. 2005; 24:3504–3515. [PubMed: 16163386]

21. Lugert S, Basak O, Knuckles P, et al. Quiescent and active hippocampal neural stem cells with distinct morphologies respond selectively to physiological and pathological stimuli and aging. Cell Stem Cell. 2010; 6:445–456. [PubMed: 20452319]

22. Andreu-Agullo C, Morante-Redolat JM, Delgado AC, et al. Vascular niche factor PEDF modulates Notch-dependent stemness in the adult subependymal zone. Nat Neurosci. 2009; 12:1514–1523. [PubMed: 19898467]

23. Basak O, Giachino C, Fiorini E, et al. Neurogenic subventricular zone stem/progenitor cells are Notch1-dependent in their active but not quiescent state. J Neurosci. 2012; 32:5654–5666. [PubMed: 22514327]

24. Tchorz JS, Suply T, Ksiazek I, et al. A modified RMCE-compatible Rosa26 locus for the expression of transgenes from exogenous promoters. Plos One. 2012; 7:e30011. [PubMed: 22253858]
25. Lugert S, Vogt M, Tchorz JS, et al. Homeostatic neurogenesis in the adult hippocampus does not involve amplification of Ascl1(high) intermediate progenitors. Nat Commun. 2012; 3:670. [PubMed: 22334073]
26. Hirrlinger PG, Scheller A, Braun C, et al. Temporal control of gene recombination in astrocytes by transgenic expression of the tamoxifen-inducible DNA recombinase variant CreERT2. Glia. 2006; 54:11–20. [PubMed: 16575885]
27. Srinivas S, Watanabe T, Lin CS, et al. Cre reporter strains produced by targeted insertion of EYFP and ECFP into the ROSA26 locus. BMC Dev Biol. 2001; 1:4. [PubMed: 11299042]
28. Merkle FT, Mirzadeh Z, Alvarez-Buylla A. Mosaic organization of neural stem cells in the adult brain. Science. 2007; 317:381–384. [PubMed: 17615304]
29. Jackson EL, Garcia-Verdugo JM, Gil-Perotin S, et al. PDGFR alpha-positive B cells are neural stem cells in the adult SVZ that form glioma-like growths in response to increased PDGF signaling. Neuron. 2006; 51:187–199. [PubMed: 16846854]
30. Bancroft, JD.; Gamble, M. Theory and Practice of Histological Techniques. Edinburgh: Churchill Livingstone; 2008.
31. Kohwi M, Petryniak MA, Long JE, et al. A subpopulation of olfactory bulb GABAergic interneurons is derived from Emx1- and Dlx5/6-expressing progenitors. J Neurosci. 2007; 27:6878–6891. [PubMed: 17596436]
32. Willaime-Morawek S, van der Kooy D. Cortex- and striatum- derived neural stem cells produce distinct progeny in the olfactory bulb and striatum. Eur J Neurosci. 2008; 27:2354–2362. [PubMed: 18445225]
33. Ventura RE, Goldman JE. Dorsal radial glia generate olfactory bulb interneurons in the postnatal murine brain. J Neurosci. 2007; 27:4297–4302. [PubMed: 17442813]
34. Young KM, Fogarty M, Kessaris N, et al. Subventricular zone stem cells are heterogeneous with respect to their embryonic origins and neurogenic fates in the adult olfactory bulb. J Neurosci. 2007; 27:8286–8296. [PubMed: 17670975]
35. Neumeister B, Grabosch A, Basak O, et al. Neural progenitors of the postnatal and adult mouse forebrain retain the ability to self-replicate, form neurospheres and undergo multipotent differentiation in vivo. Stem Cells. 2008; 27:714–723. [PubMed: 19096037]
36. Doetsch F, Petreanu L, Caille I, et al. EGF converts transit-amplifying neurogenic precursors in the adult brain into multipotent stem cells. Neuron. 2002; 36:1021–1034. [PubMed: 12495619]
37. Basak O, Taylor V. Stem cells of the adult mammalian brain and their niche. Cell Mol Life Sci. 2009; 66:1057–1072. [PubMed: 19011753]
38. Ponti G, Obernier K, Guinto C, et al. Cell cycle and lineage progression of neural progenitors in the ventricular-subventricular zones of adult mice. Proc Natl Acad Sci USA. 2013; 110:1045–1054.
39. Conover JC, Shook BA. Aging of the sub-ventricular zone neural stem cell niche. Aging Dis. 2011; 2:49–63. [PubMed: 22396866]
40. Lui JH, Hansen DV, Kriegstein AR. Development and evolution of the human neocortex. Cell. 2011; 146:18–36. [PubMed: 21729779]
41. Sanai N, Nguyen T, Ihrie RA, et al. Corridors of migrating neurons in the human brain and their decline during infancy. Nature. 2011; 478:382–386. [PubMed: 21964341]
42. Anthony TE, Mason HA, Gridley T, et al. Brain lipid-binding protein is a direct target of Notch signaling in radial glial cells. Genes Dev. 2005; 19:1028–1033. [PubMed: 15879553]
43. Alvarez-Buylla A, Garcia-Verdugo JM, Tramontin AD. A unified hypothesis on the lineage of neural stem cells. Nat Rev Neurosci. 2001; 2:287–293. [PubMed: 11283751]
44. Kageyama R, Ohtsuka T, Shimojo H, et al. Dynamic regulation of Notch signaling in neural progenitor cells. Curr Opin Cell Biol. 2009; 21:733–740. [PubMed: 19783418]
45. Fuchs E. The tortoise and the hair: Slow-cycling cells in the stem cell race. Cell. 2009; 137:811–819. [PubMed: 19490891]

46. Li L, Clevers H. Coexistence of quiescent and active adult stem cells in mammals. Science. 2010; 327:542–545. [PubMed: 20110496]
47. Wilson A, Laurenti E, Oser G, et al. Hematopoietic stem cells reversibly switch from dormancy to self-renewal during homeostasis and repair. Cell. 2008; 135:1118–1129. [PubMed: 19062086]
48. Encinas JM, Michurina TV, Peunova N, et al. Division-coupled astrocytic differentiation and age-related depletion of neural stem cells in the adult hippocampus. Cell Stem Cell. 2011; 8:566–579. [PubMed: 21549330]
49. Hattiangady B, Shetty AK. Aging does not alter the number or phenotype of putative stem/progenitor cells in the neurogenic region of the hippocampus. Neurobiol Aging. 2008; 29:129–147. [PubMed: 17092610]
50. Shook BA, Manz DH, Peters JJ, et al. Spatiotemporal changes to the subventricular zone stem cell pool through aging. J Neurosci. 2012; 32:6947–6956. [PubMed: 22593063]
51. Molofsky AV, Slutsky SG, Joseph NM, et al. Increasing p16INK4a expression decreases forebrain progenitors and neurogenesis during ageing. Nature. 2006; 443:448–452. [PubMed: 16957738]
52. Carlen M, Meletis K, Goritz C, et al. Forebrain ependymal cells are Notch-dependent and generate neuroblasts and astrocytes after stroke. Nat Neurosci. 2009; 12:259–267. [PubMed: 19234458]
53. Storch J, Thumser AE. Tissue-specific functions in the fatty acid-binding protein family. J Biol Chem. 2010; 285:32679–32683. [PubMed: 20716527]
54. Matsumata M, Sakayori N, Maekawa M, et al. The effects of Fabp7 and Fabp5 on postnatal hippocampal neurogenesis in the mouse. Stem Cells. 2012; 30:1532–1543. [PubMed: 22581784]
55. Arai Y, Funatsu N, Numayama-Tsuruta K, et al. Role of Fabp7, a downstream gene of Pax6, in the maintenance of neuroepithelial cells during early embryonic development of the rat cortex. J Neurosci. 2005; 25:9752–9761. [PubMed: 16237179]
56. Knobloch M, Braun SM, Zurkirchen L, et al. Metabolic control of adult neural stem cell activity by Fasn-dependent lipogenesis. Nature. 2013; 493:226–230. [PubMed: 23201681]
57. Bonaguidi MA, Wheeler MA, Shapiro JS, et al. In vivo clonal analysis reveals self-renewing and multipotent adult neural stem cell characteristics. Cell. 2011; 145:1142–1155. [PubMed: 21664664]

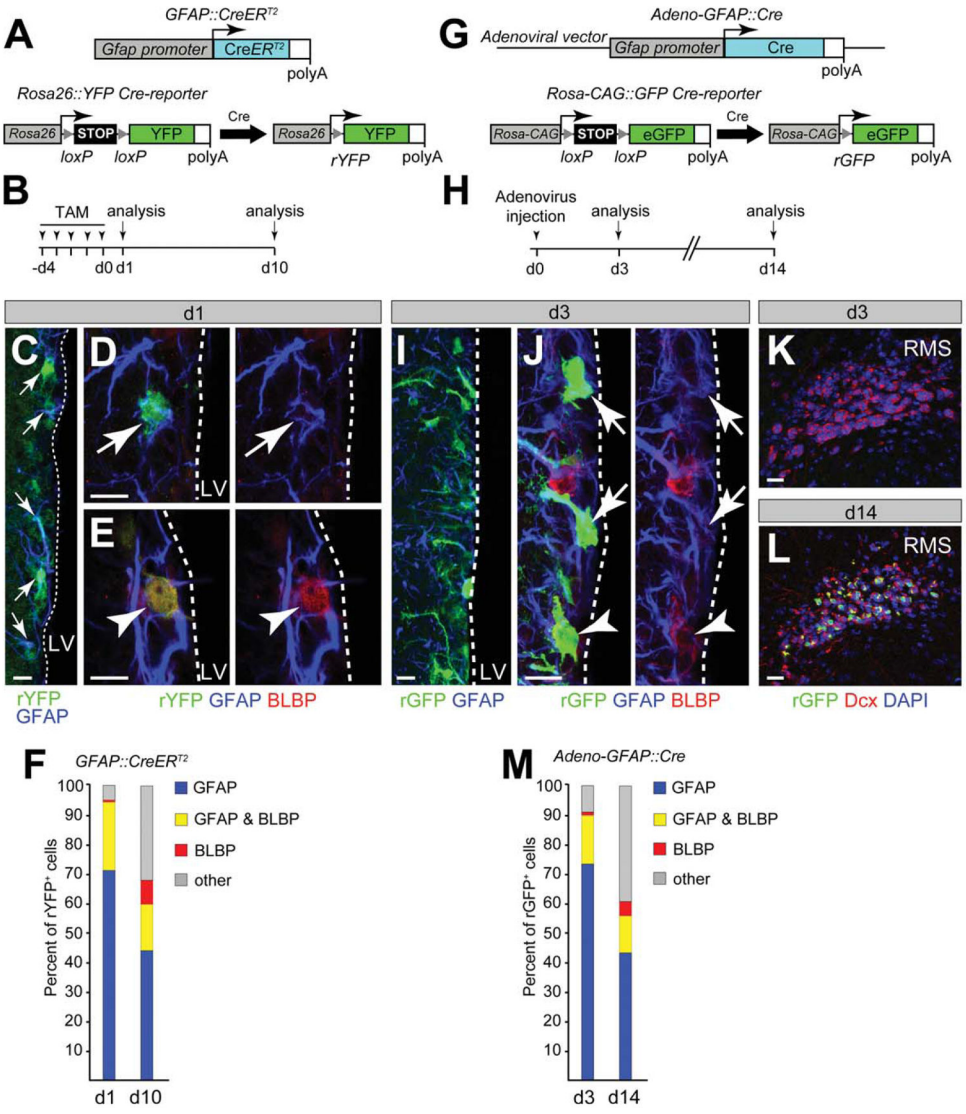

Figure 1.

GFAP$^+$ neural stem cells (NSCs) in the adult ventricular domain of subventricular zone (V-SVZ) are a heterogeneous population and can generate BLBP$^+$GFAP$^-$ cells. **(A):** Genetic labeling of GFAP$^+$ cells in the adult V-SVZ. *GFAP::CreER^{T2}* construct driving expression of TAM-inducible CreER^{T2}-recombinase from the GFAP promoter. *GFAP::CreER^{T2}* transgenic mice were crossed with mice carrying a *Rosa-YFP* (rYFP) inducible reporter allele. Upon TAM induction, CreER^{T2} is activated in GFAP$^+$ cells and recombines the *Rosa26::YFP* reporter locus, thereby genetically labeling GFAP$^+$ cells with rYFP expression. **(B):** *GFAP::CreER^{T2}* mice were injected with TAM for five consecutive days (arrowheads) and analyzed after 1- and 10-day chase periods. **(C):** Recombined rYFP$^+$ V-SVZ cells (arrows) expressed GFAP at day 1 after TAM induction. **(D, E):** rYFP$^+$ cells expressed GFAP but not BLBP (arrows) or both GFAP and BLBP (arrowheads) at day 1 after TAM induction. **(F):** The majority of recombined rYFP$^+$ V-SVZ cells expressed GFAP (blue) or GFAP and BLBP (yellow) at day 1 after TAM induction. Genetically labeled

GFAP$^+$ cells generated BLBP$^+$GFAP$^-$ cells (red) as well as transient amplifying progenitors (TAPs) and neuroblasts (gray, "other") at day 10 after TAM induction. **(G):** Adenoviral *GFAP::Cre* construct driving expression of Cre recombinase from the mouse GFAP promoter. Upon adenoviral infection, Cre recombines the *Rosa-CAG::GFP* reporter locus in GFAP$^+$ V-SVZ cells, thereby genetically labeling NSCs with rGFP expression. **(H):** *Rosa-CAG::GFP* mice were injected intracerebroventricular with Adeno-GFAP::Cre and analyzed after 3- and 14-day chases. **(I):** Recombined rGFP$^+$ V-SVZ cells expressed GFAP at day 3 postinfection. **(J):** Many rGFP$^+$ cells expressed GFAP but not BLBP (arrows) and some expressed both GFAP and BLBP (arrowheads) at day 3 postinfection. **(K, L):** Genetically labeled GFAP$^+$ cells generated rGFP$^+$ migratory neuroblasts that invaded the RMS at day 14 but were not present at day 3 postinfection. **(M):** The majority of the recombined rGFP$^+$ V-SVZ cells expressed GFAP (blue) or GFAP and BLBP (yellow) at day 3 postinfection. Lineage analysis revealed that genetically labeled GFAP$^+$ cells generated BLBP$^+$GFAP$^-$ cells (red) as well as TAPs and neuroblasts (gray, "other") at day 14 postinfection. Dashed lines mark the lining of the LV. Scale bars =10 μm. Abbreviations: BLBP, brain lipid binding protein; DAPI, 4′,6-diamidino-2-phenylindole; GFAP, glial fibrillary acidic protein; GFP, green fluorescent protein; LV, lateral ventricle; RMS, rostral migratory stream; TAM, Tamoxifen.

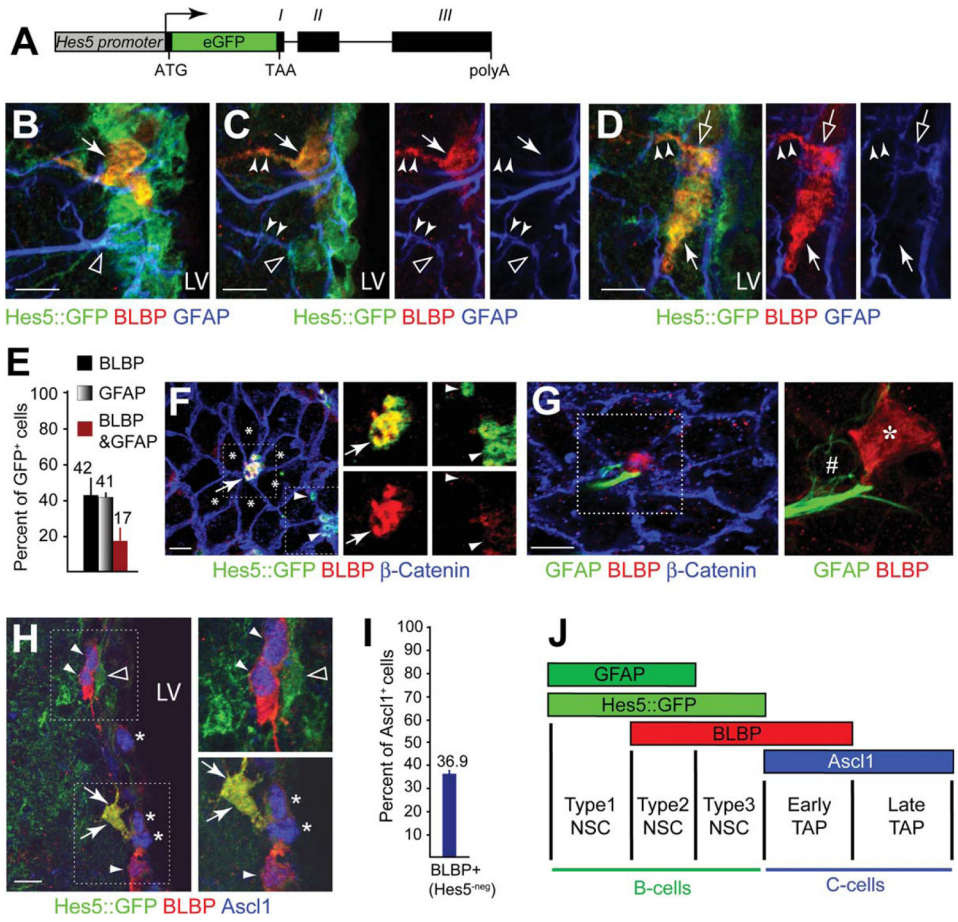

Figure 2.

Hes5^{+} NSCs are a heterogeneous population that expresses GFAP and/or BLBP. **(A):** *Hes5::GFP* construct driving expression of GFP from the mouse *Hes5* regulatory elements including promoter, exons I, II, III, introns, the endogenous 3′-untranslated region, and polyA [16]. **(B):** *Hes5::GFP*$^{+}$ ventricular domain of subventricular zone (V-SVZ) cells express GFAP (open arrowhead) and/or BLBP (arrow) and show a radial morphology. **(C, D):** *Hes5::GFP*$^{+}$ cells express GFAP (open arrowheads), BLBP (filled arrows), or both (open arrows). Note cells belonging to each of these subpopulations bear radial processes (filled arrowheads). **(E):** Quantification of the proportion of V-SVZ *Hes5*$^{+}$ cells that express GFAP, BLBP, or both GFAP and BLBP. **(F):** *Hes5*$^{+}$ cells project through pinwheel structures in the ependymal wall. Some pinwheels contain *Hes5*$^{+}$BLBP^{+} NSCs (arrow) others *Hes5*$^{+}$BLBP^{-} NSCs (arrowheads). Note that ependymal cells (asterisks) express neither *Hes5* nor BLBP. **(G):** Pinwheel structures in the ependymal wall contain GFAP^{+} and BLBP^{+} NSCs. Some pinwheels have both GFAP^{+} and BLBP^{+} NSCs projecting to the ventricle. Inset is a 3D reconstruction showing the cell bodies of the two cells (one GFAP^{+} #, one BLBP^{+} * NSC) projecting through the pinwheel shown in (G). **(H):** *Hes5*$^{+}$BLBP^{+} (arrows) and *Hes5*$^{+}$BLBP^{-} NSCs (open arrowhead) do not express the proneural TAP protein Ascl1. TAPs express Ascl1 (asterisks) or Ascl1 and BLBP (filled arrowheads) but not in combination with *Hes5*. **(I):** Composition of the TAP in the V-SVZ and overlap with

BLBP expression. BLBP^{+}*Hes5*$^{-}$ cells represent a fraction of Ascl1^{+} TAPs (36.9%) and are distinct from *Hes5*$^{+}$BLBP^{+} NSCs. **(J):** Composition of NSC and TAP populations in the V-SVZ based on quantification of marker expression. NSCs (B cells) express *Hes5* (dark green) and can be subdivided into GFAP^{+} (light green) or BLBP^{+} (red) subpopulations that partially overlap. BLBP expression is maintained in a proportion of Ascl1^{+} TAPs (C cells). The remaining TAPs express Ascl1 but neither BLBP nor *Hes5*. Quantifications are shown as mean ±SD. Scale bars =10 μm. Abbreviations: BLBP, brain lipid binding protein; GFP, green fluorescent protein; GFAP, glial fibrillary acidic protein; LV, lateral ventricle; NSCs, neural stem cells; polyA, polyadenylation signal; TAP, transient amplifying progenitors.

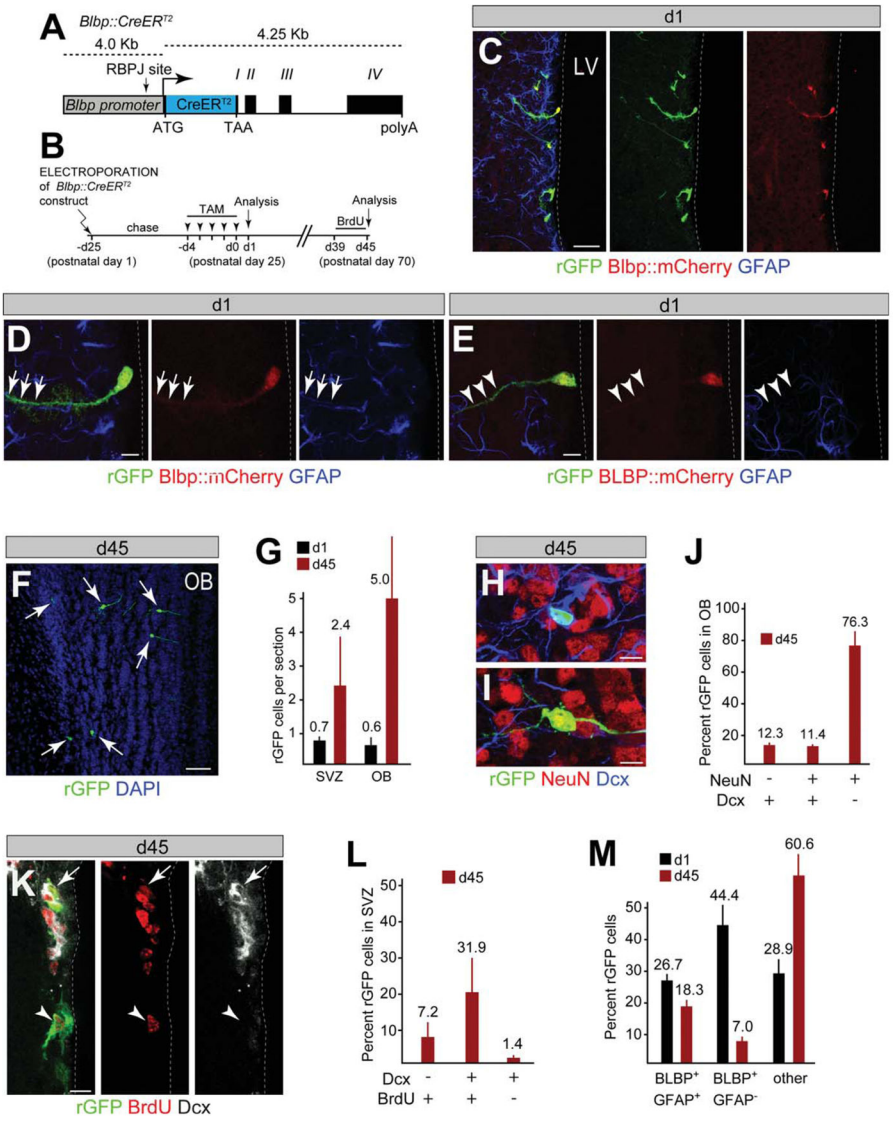

Figure 3.

BLBP$^+$ cells include a long-term neurogenic population. **(A):** *Blbp::CreER^{T2}* construct driving expression of TAM-inducible CreER^{T2}-recombinase from the mouse *Blbp* regulatory elements including promoter exons I, II, III, IV, introns, the endogenous 3-′untranslated region, and polyA. **(B):** *Blbp::CreER^{T2}* expressing cells were lineage traced by electroporation of the *Blbp::CreER^{T2}* and *Blbp::mCherry* constructs into the cells of LV wall of postnatal day 1 *Rosa-CAG::GFP* mice followed by TAM induction after 20 days and analysis 1 and 45 days later. BrdU was administered in the drinking water for 1 week before analysis at day 45. **(C):** Immediately after TAM administration (d1) sparse recombined (rGFP$^+$) cells appeared in the V-SVZ and many had a radial glial morphology and expressed *Blbp::mCherry*. **(D):** Some rGFP$^+$*Blbp::mCherry*$^+$ cells in the V-SVZ had the polarized radial morphology typical of adult neural stem cells (NSCs) and expressed GFAP within their radial process (arrows) at day 1. **(E):** Some rGFP$^+$*Blbp::mCherry*$^+$ cells in the V-SVZ did not express GFAP but showed a radial morphology (arrowheads) at day 1. **(F):** 45 days

after TAM induction, *Blbp::CreER^{T2}*-derived rGFP^{+} cells had generated progeny that dispersed into the neuronal layers of the OB (arrows). **(G):** Quantification of *Blbp::CreER^{T2}* progeny (rGFP^{+}) in the V-SVZ and OB depicted as the number of rGFP^{+} cells per section at day 1 and day 45 after TAM induction. The rGFP^{+} population expanded in the V-SVZ and accumulated in the OB, indicating that the initially targeted BLBP^{+} cells generated multiple progeny over time. **(H, I):** *Blbp::CreER^{T2}* cells generated neuroblasts (H, Dcx^{+}) and neurons (I, NeuN^{+}) in the OB 45 days after TAM induction. **(J):** Quantification of the phenotype of rGFP^{+} cells in the OB 45 days (d45) after TAM injection. *Blbp::CreER^{T2}* derived rGFP^{+} cells in the OB were neuroblasts (Dcx^{+}), differentiating neurons (NeuN^{+}Dcx^{+}), or mature neurons (NeuN^{+}). **(K):** *Blbp::CreER^{T2}*-derived cells (rGFP^{+}) remained mitotically active in the V-SVZ 45 days after TAM induction (BrdU^{+}, arrowheads) and generated new neuroblasts (Dcx^{+}BrdU^{+}, arrows). **(L):** Quantification of proliferating progenitors (BrdU^{+}), proliferating neuroblasts (Dcx^{+}BrdU^{+}), and neuroblasts (Dcx^{+}) among rGFP^{+} cells in the V-SVZ 45 days after TAM induction. **(M):** Quantification of the phenotype of rGFP^{+} cells in the V-SVZ 1 day (black bars) or 45 days (red bars) after TAM injection. At day 1, most of rGFP^{+} cells coexpressed *Blbp::mCherry*$^{+}$ and GFAP or were *Blbp::mCherry*$^{+}$ but GFAP^{-}. At day 45, the proportion of BLBP^{+} cells decreased while that of their progeny ("other," transient amplifying progenitors and neuroblasts) proportionally increased. Dashed lines mark the lining of the lateral ventricle. All quantifications are show as mean ±SD. Scale bars =10 μm; in (C, F) =50 μm. Abbreviations: BrdU, 5-bromo deoxyuridine; BLBP, brain lipid binding protein; DAPI, 4′,6-diamidino-2-phenylindole; GFP, green fluorescent protein; GFAP, glial fibrillary acidic protein; LV, lateral ventricle; OB, olfactory bulb; polyA, polyadenylation signal; SVZ, subventricular zone; TAM, Tamoxifen.

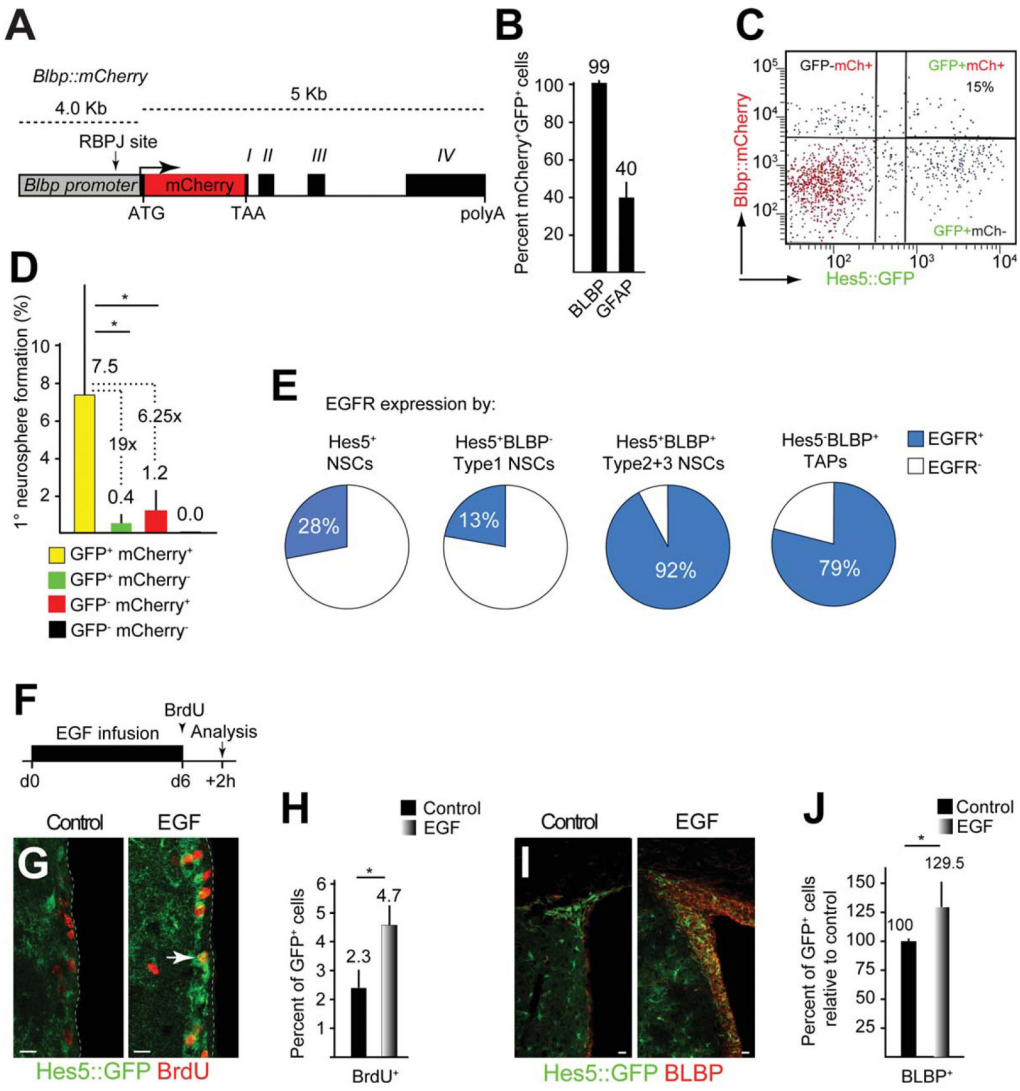

Figure 4.

Hes5^{+}BLBP^{+} cells are EGF-responsive active NSCs. **(A):** *Blbp::mCherry* construct driving expression of mCherry from the mouse *Blbp* regulatory elements including promoter, exons I–IV, introns, the endogenous 3-′untranslated region, and polyA. **(B):** Quantification of BLBP and GFAP protein expression among *Hes5::GFP*$^{+}$*Blbp::mCherry*$^{+}$ NSCs. All *Hes5::GFP*$^{+}$*Blbp::mCherry*$^{+}$ cells express BLBP protein and some express GFAP. **(C):** Fluorescence activated cell sorting (FACS) analysis and purification of *Hes5::GFP*$^{+}$ and *Blbp::mCherry*$^{+}$ ventricular domain of subventricular zone (V-SVZ) cells. *Hes5::GFP*$^{+}$*Blbp::mCherry*$^{+}$ NSCs are 15% of the total fluorescent populations in the V-SVZ. **(D):** Quantification of neurosphere formation of FACSed *Hes5::GFP*$^{+}$ and *Blbp::mCherry*$^{+}$ cell populations. Fold enrichment in neurosphere formation of the GFP^{+}mCherry^{+} population relative to single positive populations. The *Hes5::GFP*$^{+}$*Blbp::mCherry*$^{+}$ population is enriched in colony forming cells in vitro. *Hes5::GFP*$^{-}$*Blbp::mCherry*$^{-}$ cells did not form neurospheres. **(E):** Quantitative FACS analysis of EGFR expression (fluorescently-labeled EGF binding) by the *Hes5::GFP*$^{+}$ and

Blbp::mCherry$^+$ cell populations sorted directly from the adult V-SVZ. EGF binding within the *Hes5*$^+$ NSC population correlates with the *BLBP* expression. *Hes5*$^+$BLBP$^+$ cells represent a major EGF responsive NSC fraction. **(F):** EGF was infused into a lateral ventricle of adult mice adjacent to the V-SVZ for 6 days and BrdU administered 2 hours prior to analysis. **(G):** EGF infusion increased BrdU incorporation in the V-SVZ including by *Hes5*$^+$ NSCs (arrow) compared to saline-infused control animals. **(H):** Quantification of the increase in BrdU$^+$ cells among the *Hes5*$^+$ population in EGF-infused mice compared to saline-infused control mice. **(I, J):** EGF infusion increased BLBP$^+$ cells, including *Hes5*$^+$BLBP$^+$ NSCs, in the V-SVZ. Dashed lines mark the lining of the lateral ventricle. All quantifications are show as mean ±SD. *, Student's *t* test $p < .05$. Scale bars =10 μm. Abbreviations: BrdU, 5-bromo deoxyuridine; BLBP, brain lipid binding protein; EGF, epidermal growth factor; EGFR, epidermal growth factor receptor; GFP, green fluorescent protein; GFAP, glial fibrillary acidic protein; NSCs, neural stem cells; PolyA, polyadenylation signal; TAPs, transient amplifying precursors.

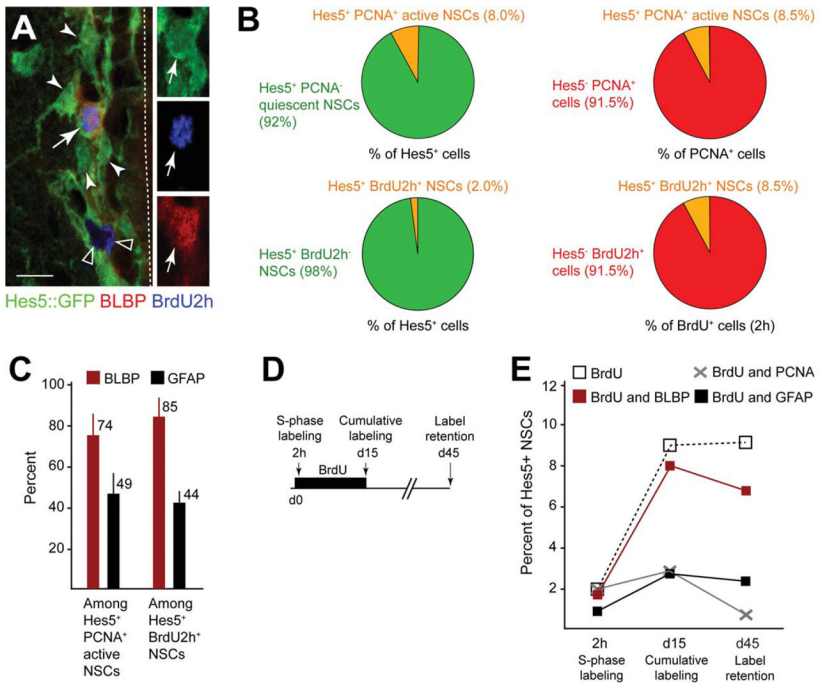

Figure 5.

Hes5^{+}BLBP^{+} cells include active NSCs in vivo. **(A):** Very few *Hes5::GFP*$^{+}$ NSCs incorporate BrdU after a short 2-hour pulse (arrows) and most of them are quiescent (filled arrowheads). The majority of BrdU^{+} cells do not express *Hes5* (open arrowheads) and include transient amplifying precursors and neuroblasts. BrdU-incorporating *Hes5::GFP*$^{+}$ NSCs express BLBP (arrows). Dashed line marks the lining of the lateral ventricle. **(B):** Quantification of the overlap between the *Hes5::GFP*$^{+}$ NSC population and proliferation markers. Only a small fraction of *Hes5::GFP*$^{+}$ NSCs are actively proliferating (PCNA^{+}) or in S-phase (BrdU 2-hour pulse). Proliferating *Hes5::GFP*$^{+}$ NSCs represent a small fraction of all dividing cells in the V-SVZ. **(C):** Quantification of BLBP and GFAP expression by actively proliferating *Hes5::GFP*$^{+}$ NSC. Most dividing *Hes5::GFP*$^{+}$ cells express BLBP and a fraction of them express GFAP. **(D):** Scheme of BrdU-labeling paradigms used to address mitotic activity of *Hes5*$^{+}$ NSCs in the V-SVZ. A short 2h BrdU pulse was used to label cells in S-phase. BrdU was administered for 15 days with the drinking water to cumulatively label slowly dividing NSCs. Label-retaining cells were analyzed at day 45 after 15 days of BrdU label and 30 days chase period. **(E):** BLBP expression in *Hes5*$^{+}$ NSCs correlates with both mitotic activity and label retention. Few *Hes5*$^{+}$ NSCs incorporated BrdU during a 2-hour pulse (2h). *Hes5*$^{+}$ NSCs that incorporated BrdU after a 15-day labeling (d15) retained the label over 30 days of chase (d45). The majority of the BrdU-labeled cells exited the cell cycle and became quiescent (PCNA^{-}). Many BrdU incorporating and BrdU label-retaining *Hes5*$^{+}$ NSCs expressed BLBP and a proportion also expressed GFAP. Scale bar =10 μm. Abbreviations: BrdU, 5-bromo deoxyuridine; BLBP, brain lipid binding protein; GFP, green fluorescent protein; GFAP, glial fibrillary acidic protein; NSCs, neural stem cells; PCNA, proliferating cell nuclear antigen.

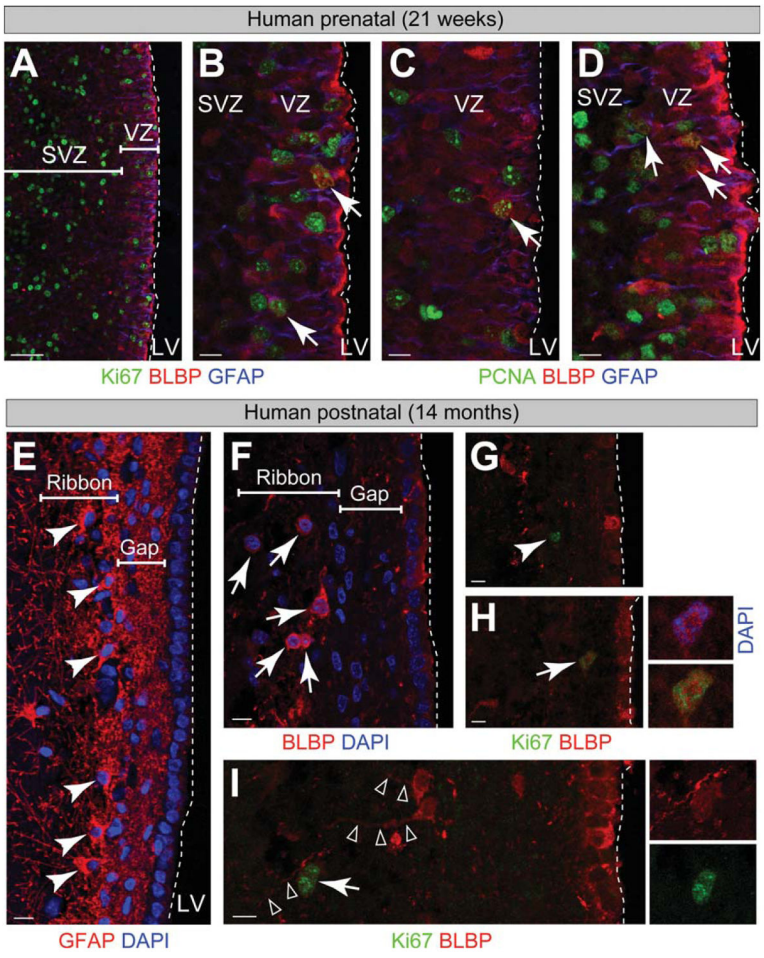

Figure 6.

BLBP$^+$ putative neural stem cells (NSCs) in the prenatal and postnatal human brain. (**A–D):** BLBP$^+$ cells that proliferate (Ki67$^+$ or PCNA$^+$, arrows) represent a fraction of the dividing cells in the human prenatal brain (week 21). BLBP$^+$ cells are preferentially found in the VZ where most radial glia cell bodies reside at this stage. **(E):** After birth, the VZ/V-SVZ transform into a hypocellular gap region and an astrocyte ribbon where cell bodies of GFAP$^+$ NSCs reside (arrowheads). **(F):** BLBP$^+$ cells (arrows) cluster in the astrocyte ribbon. **(G–I):** Fewer proliferating Ki67$^+$ cells are present in the human postnatal neurogenic region than in the prenatal brain. Some Ki67$^+$ cells in the human postnatal VZ/V-SVZ express BLBP (arrows) and others are BLBP negative (filled arrowhead). Some BLBP$^+$ cells of the astrocyte ribbon have a radial process (open arrowheads). Dashed lines mark the lining of the lateral ventricle. Scale bars =10 μm; (A) =50 μm. Abbreviations: BLBP, brain lipid binding protein; DAPI, 4′,6-diamidino-2-phenylindole; GFAP, glial fibrillary acidic protein; PCNA, proliferating cell nuclear antigen; LV, lateral ventricle, SVZ, subventricular zone; VZ, ventricular zone.

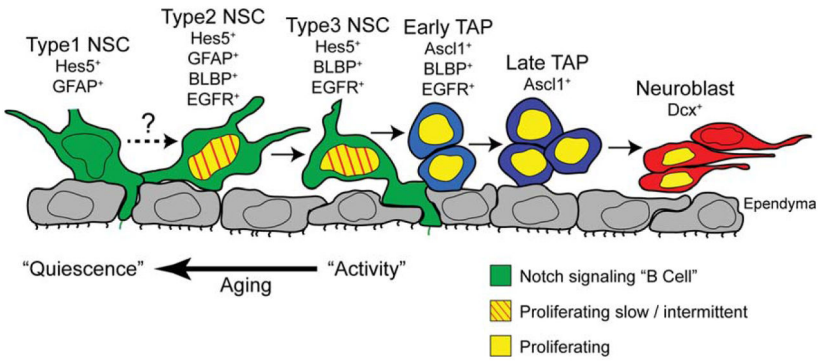

Figure 7.

NSC diversity in the adult subventricular zone (SVZ). Summary and model of NSC and progenitor heterogeneity in the adult SVZ neurogenic lineage. Adult SVZ NSCs are Notch-dependent and express the canonical Notch target gene *Hes5* (green cells). The *Hes5*$^+$ NSC pool is subdivided into GFAP$^+$ type 1, GFAP$^+$BLBP$^+$ type 2, and BLBP$^+$ type 3 populations which all show radial glia-like features and contact the lateral ventricles through ependymal pinwheel structures. Type 2 cells likely generate type 3 cells but the lineage relationship with type 1 cells under normal conditions in vivo remains unclear. BLBP$^+$ type 2 and type 3 subpopulations do not express TAP markers (Ascl1) but express the EGF receptor and, in agreement, include most of the proliferating *Hes5*$^+$ NSCs. By comparison, type 1 NSCs are mitotically inactive. Type 2 and type 3 NSCs are reduced with age, and this reduction correlates with reduced neurogenesis, reduced mitotic activity and a shift toward type 1 NSCs. TAPs express Ascl1 but not *Hes5* and are also heterogeneous based on the expression of BLBP. Abbreviations: BLBP, brain lipid binding protein; EGFR, epidermal growth factor receptor; GFAP, glial fibrillary acidic protein; NSCs, neural stem cells; TAP, transient amplifying progenitors.